Computers and Concrete, *Vol. 12, No. 1 (2013) 19-36*
DOI: http://dx.doi.org/10.12989/cac.2013.12.1.019

Modelling dowel action of discrete reinforcing bars for finite element analysis of concrete structures

A.K.H. Kwan* and P.L. Ng[a]

Department of Civil Engineering, The University of Hong Kong, Pokfulam Road, Hong Kong, China

(Received August 15, 2011, Revised February 2, 2012, Accepted April 16, 2012)

Abstract. In the finite element analysis of reinforced concrete structures, discrete representation of the steel reinforcing bars is considered advantageous over smeared representation because of the more realistic modelling of their bond-slip behaviour. However, there is up to now limited research on how to simulate the dowel action of discrete reinforcing bars, which is an important component of shear transfer in cracked concrete structures. Herein, a numerical model for the dowel action of discrete reinforcing bars is developed. It features derivation of the dowel stiffness based on the beam-on-elastic-foundation theory and direct assemblage of the dowel stiffness matrix into the stiffness matrices of adjoining concrete elements. The dowel action model is incorporated in a nonlinear finite element program based on secant stiffness formulation and application to deep beams tested by others demonstrates that the incorporation of dowel action can improve the accuracy of the finite element analysis.

Keywords: cracking; dowel action; finite element analysis; reinforced concrete

1. Introduction

Compared to the axial and flexural counterparts, the shear behaviour of concrete structures is less predictable, due to the complexity of shear transfer mechanisms and the difficulties in numerical modelling, and yet it plays an important role in the overall structural behaviour of reinforced concrete members (Bresler and Scordelis 1963). Park and Paulay (1975) suggested that the shear resistance of a cracked concrete structure is constituted of: (1) direct transfer of shear force by uncracked concrete; (2) direct tensile forces in stirrups; (3) aggregate interlock at crack surfaces; and (4) dowel action of reinforcing bars crossing the cracks. Fig. 1 illustrates the above internal forces inside a cracked concrete beam. Although often ignored, the dowel action of reinforcing bars is definitely an important component of shear transfer in a cracked concrete member. Its relative importance depends on several factors, including the geometry of the concrete member, the reinforcement layout, the material properties and the crack pattern.

Being a major component of shear transfer, the dowel action of reinforcing bars has been investigated experimentally by a number of researchers (Krefeld and Thurston 1966, Dulacska 1972, Jimenez *et al*. 1979, Millard and Johnson 1984, Vintzeleou and Tassios 1986, 1987,

*Corresponding author, Professor, E-mail: khkwan@hku.hk
[a]Honorary Research Associate, E-mail: irdngpl@gmail.com

http://www.techno-press.org/?journal=cac&subpage=8 ISSN: 1598-8198(Print), 1598-818X (Online)

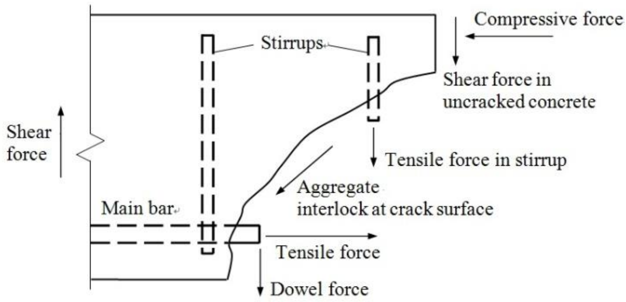

Fig. 1 Internal forces in a cracked beam

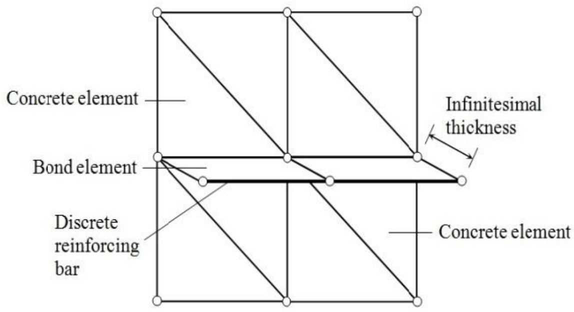

Fig. 2 Bond element

Soroushian *et al*. 1986, 1987, 1988, Pruijssers 1988, Dei Poli *et al*. 1992, 1993, Mannava *et al*. 1999). However, despite decades of research on finite element analysis of reinforced concrete structures, there has been basically no explicit consideration of the dowel action in finite element modelling (Kwak and Kim 2004, Hassan Dirar and Morley 2005, Oliveira *et al*. 2008, Pimentel *et al*. 2008, Kazaz 2011, Yu *et al*. 2011). At the most, a gross allowance was made by lumping the dowel action with other components of shear transfer (ASCE 1982). Nevertheless, some years ago, a dowel action model for application with smeared representation of reinforcing bars has been developed (He and Kwan 2001). In this model, the dowel force and deformation are expressed in smeared forms and the dowel stiffness matrix is assembled into the concrete element stiffness matrix. It has been applied to analyse deep and coupling beams with certain degree of success (He 1999, Zhao *et al*. 2004, El-Ariss 2007).

The modelling of dowel action for smeared reinforcement is only an interim measure so as to be compatible with the existing finite element programs using smeared representation of the reinforcing bars. In the long run, for more realistic modelling of the bond-slip behaviour and dowel action of the reinforcing bars, discrete representation of the reinforcing bars should be adopted instead of smeared representation. One reason is that to account for the bond-slip behaviour, the reinforcing bars have to be treated as individual bars and should not be simply smeared into the concrete. Another reason is that the dowel action pushing against the concrete core and the dowel action pushing against the concrete cover are not quite the same. In the former case, the concrete core acts like an elastic foundation for the dowel bars whereas in the later case, the dowel bars tend to peel off the concrete cover and are actually supported by the stirrups (Soroushian *et al*. 1986, 1987). With the reinforcing bars smeared into the concrete, it is difficult to differentiate between these two actions. The only way to properly model these actions is to treat the reinforcing bars as discrete bars.

With discrete representation, the reinforcing bars are modelled by discrete one-dimensional steel bar or frame elements. To model the bond-slip behaviour of the reinforcing bars, the steel elements are connected to the concrete through bond elements, which simulate the bond-slip behaviour of the steel-concrete interface. A commonly used bond element is the 4-noded interface element developed by Goodman *et al*. (1968), as depicted in Fig. 2. Each such bond element is assumed to have infinitesimal thickness. It has two pairs of duplicated nodes. The duplicated nodes in each pair have the same coordinates but independent degrees of freedom. Among them, one is connected to the steel reinforcement while the other is connected to the concrete. The difference in displacement of the duplicated nodes along the steel-concrete interface is taken as the slip.

In theory, to model the dowel action of the reinforcing bars, the steel elements modelling the reinforcing bars are required to have flexural stiffness. For this reason, the reinforcing bars have to be modelled by frame elements having at each node two translational degrees of freedom and one rotational degree of freedom. Herein, a numerical method of incorporating the dowel stiffness of the reinforcing bars into the adjoining concrete elements so that the steel elements do not need to have flexural stiffness and therefore can be in the form of the simpler bar elements with no rotational degree of freedom is proposed.

2. Modelling of concrete, steel reinforcement and bond

2.1 Modelling of concrete

The concrete is modelled by 3-noded triangular plane stress elements for two-dimensional analysis. Before cracking, the principal directions are taken as the coordinate axes of the local coordinate system. After cracking, the crack directions (the directions perpendicular to and parallel to the crack plane) are taken as the coordinate axes of the local coordinate system. Once the concrete has cracked, the crack directions are fixed and not allowed to rotate.

To account for the biaxial behaviour, the biaxial stress-strain relation is described via equivalent uniaxial strains, which are defined by

$$\varepsilon_{e1} = \frac{1}{1-v_1 v_2}\left(\varepsilon_1 + v_2\varepsilon_2\right) \tag{1a}$$

$$\varepsilon_{e2} = \frac{1}{1-v_1 v_2}\left(\varepsilon_2 + v_1\varepsilon_1\right) \tag{1b}$$

where ε_{e1} and ε_{e2} are the equivalent uniaxial strains, ε_1 and ε_2 are the principal strains, v_1 and v_2 are the Poisson's ratios, and the subscripts 1 and 2 denote quantities in the major and minor principal directions, respectively. For the sign convention, tension is positive and compression is negative.

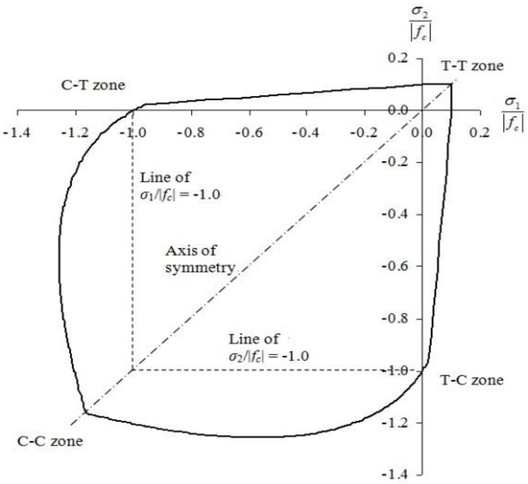

Fig. 3 Biaxial strength envelope of concrete

The principal stresses σ_1 and σ_2 are each assumed to be a single variable function of ε_{e1} and ε_{e2}, respectively, so that the biaxial stress-strain relation is effectively decomposed into two separate uniaxial stress-strain relations.

The tensile and compressive strengths in the principal directions are determined based on the biaxial strength envelope developed by Kupfer and Gerstle (1973), as illustrated in Fig. 3. The strength envelope consists of four distinct zones, namely, the tension-tension (T-T), tension-compression (T-C), compression-compression (C-C) and compression-tension (C-T) zones. For a principal direction in tension, the uniaxial stress-strain curve proposed by Guo and Zhang (1987) is adopted, with the peak tensile stress f_t replaced by the tensile strength of concrete determined from the strength envelope. For a principal direction in compression, the uniaxial stress-strain curve proposed by Saenz (1964) is adopted, with the peak compressive stress f_c replaced by the compressive strength of concrete determined from the strength envelope.

From the stress-strain curves, the principal stresses σ_1 and σ_2 are obtained, and the secant stiffness values in the two principal directions E_{c1} and E_{c2} are evaluated as $\sigma_1/\varepsilon_{e1}$ and $\sigma_2/\varepsilon_{e2}$, respectively. The constitutive matrix of concrete $[D_c']$ in the local coordinate system is derived as

$$[D_c'] = \begin{bmatrix} \dfrac{E_{c1}}{1-v_1 v_2} & \dfrac{v_2 E_{c1}}{1-v_1 v_2} & 0 \\ \dfrac{v_1 E_{c2}}{1-v_1 v_2} & \dfrac{E_{c2}}{1-v_1 v_2} & 0 \\ 0 & 0 & G \end{bmatrix} \tag{2}$$

in which G is the shear modulus. Before cracking of concrete, the shear modulus is taken as the initial elastic shear modulus G_0. After cracking, the shear modulus is taken as βG_0, in which β is a dimensionless shear retention factor ranging from 0.0 to 1.0 to account for the aggregate interlock effect. Based on the formula proposed by He and Kwan (2001) and the modification proposed by Ng (2007), the value of β is taken as

$$\beta = \beta_0 \left(1 - \frac{\varepsilon_{e1} - \varepsilon_{t0}}{30\varepsilon_{t0}}\right)^2 \tag{3}$$

where ε_{t0} is the tensile strain at peak tensile stress. Generally, as ε_{e1} increases to beyond ε_{t0}, the aggregate interlock effect gradually diminishes. The value of β_0 is taken to be 0.4, as proposed by Walraven (1980) based on experimental results.

2.2 Modelling of steel reinforcement

The steel reinforcement is modelled by 2-noded bar elements. To account for the elastic, plastic and strain hardening behaviour of the steel reinforcement, the stress-strain relation proposed by Mander (1984) is adopted. As proposed by Mander, the steel stress σ_s is related to the steel strain ε_s by

$$\sigma_s = E_{s0}\varepsilon_s \quad \text{for} \quad \varepsilon_s \le f_y / E_{s0} \tag{4a}$$

$$\sigma_s = f_y \quad \text{for} \quad f_y / E_{s0} < \varepsilon_s \le \varepsilon_{sh} \tag{4b}$$

$$\sigma_s = f_y + \left(f_u - f_y\right)\left[1 - \left(\frac{\varepsilon_u - \varepsilon_s}{\varepsilon_u - \varepsilon_{sh}}\right)^n\right] \quad \text{for} \quad \varepsilon_{sh} < \varepsilon_s \le \varepsilon_u \tag{4c}$$

where E_{s0} is the initial elastic modulus, f_y is the yield strength, f_u is the ultimate tensile strength, ε_{sh} is the strain at start of strain hardening, ε_u is the ultimate strain, and n is a coefficient depending on the strain hardening property of the steel. From the stress and strain values, the secant stiffness of the steel E_s is evaluated as σ_s/ε_s, and the constitutive matrix of steel reinforcement $[D_s']$ in the local coordinate system is derived as

$$[D_s'] = \begin{bmatrix} E_s & 0 & 0 \\ 0 & 0 & 0 \\ 0 & 0 & 0 \end{bmatrix} \tag{5}$$

2.3 Modelling of bond

The 4-noded bond element depicted in Fig. 2 is employed to model the bond between the steel reinforcement and concrete. The bond stress-slip relation follows that recommended by CEB-FIP Model Code 1990 (CEB 1993), which is given as

$$\tau_b = \tau_p \left(\frac{s_b}{s_1}\right)^{0.4} \quad \text{for} \quad s_b \le s_1 \tag{6a}$$

$$\tau_b = \tau_p \quad \text{for} \quad s_1 < s_b \le s_2 \tag{6b}$$

$$\tau_b = \left(\frac{s_b - s_2}{s_3 - s_2}\right)(\tau_f - \tau_p) + \tau_p \text{ for } \quad s_2 < s_b \le s_3 \tag{6c}$$

$$\tau_b = \tau_f \quad \text{for} \quad s_3 < s_b \tag{6d}$$

in which τ_b is the bond stress, τ_p is the peak bond stress, τ_f is the residual bond stress, s_b is the bond slip, and s_1, s_2 and s_3 are the slip at start of peak bond stress, slip at end of peak bond stress and slip at start of residual bond stress, respectively.

Initially, the secant bond stiffness k_b is taken as 200 N/mm^3, as recommended by the Model Code 1990. Then, as bond slip occurs, the bond stress τ_b is determined from the bond stress-slip relation in Eq. (6), and the secant bond stiffness k_b is evaluated as τ_b/s_b. Having obtained the secant bond stiffness, the stiffness matrix of the bond element in the local coordinate system is derived following the procedures developed by Goodman *et al*. (1968) with the area of interface taken as the length of the bond element times the total perimeter of the steel reinforcing bars.

For the concrete, steel and bond elements, upon deriving the stiffness matrices in their respective local coordinate systems, the corresponding stiffness matrices in the global coordinate system are obtained by the usual coordinate transformation.

3. Dowel force-displacement relation

Let the dowel force be denoted by V_d and the dowel displacement be denoted by Δ_d. The V_d - Δ_d relation may be derived from experiments. Based on experimental results, Dulacska (1972), Millard and Johnson (1984) and Dei Poli *et al.* (1993) recommended a linearly elastic-perfectly plastic relation, while Soroushian *et al.* (1986) suggested adding a gently descending branch to the V_d - Δ_d curve. In reality, whether the V_d - Δ_d curve should have a descending branch is dependent on the ductility of the dowel action. If the peak dowel force is attained by yielding of the dowel bars and ample restraints in the form of stirrups have been provided to sustain the dowel force at the post-peak stage, the dowel action should be ductile. Assuming that the above conditions are satisfied and the dowel action is sufficiently ductile, a linearly elastic-perfectly plastic V_d - Δ_d curve with no descending branch is adopted.

The linearly elastic-perfectly plastic dowel force-displacement relation adopted follows that of He and Kwan (2001). Mathematically, it is given by

$$V_d = k_{d0}\,\Delta_d \text{ for } \Delta_d \le \Delta_{d0} \tag{7a}$$

$$V_d = V_{d0} \text{ for } \Delta_d > \Delta_{d0} \tag{7b}$$

where k_{d0} is the initial dowel stiffness, V_{d0} is the peak dowel force (or dowel strength), and Δ_{d0} is the dowel displacement at peak dowel force. Fig. 4 depicts the dowel force-displacement curve.

The initial dowel stiffness k_{d0} may be established by treating the reinforcing bar as a beam and the surrounding concrete as an elastic foundation. According to the beam-on-elastic-foundation theory, the foundation may be modelled as a bed of Winkler springs so that the reaction force from the foundation at any point may be assumed to be proportional to the deflection of the beam at that

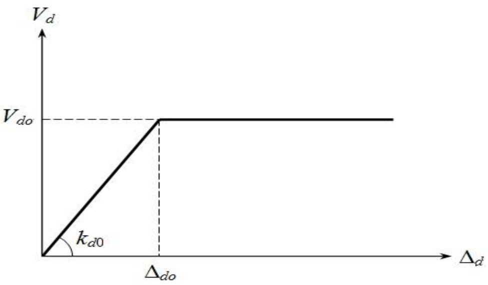

Fig. 4 Dowel force-displacement curve

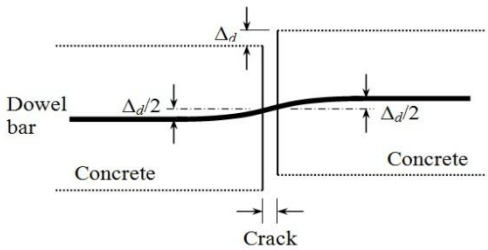

(a) Contraflexural deformation of dowel bar

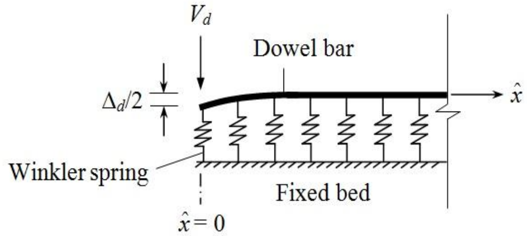

(b) Modelling of elastic foundation by Winkler springs

Fig. 5 Dowel action modelled as a beam on elastic foundation

point. Cutting the reinforcing bar at the point of contraflexure, the bar may be treated as a semi-infinite beam resting on the foundation subjected to a concentrated load V_d at one end, as shown in Fig. 5. From the analytical solution for the beam-on-elastic-foundation problem (Hetenyi 1958), the deflection of the dowel bar $\Delta_{\hat{x}}$ at any point is derived as

$$\Delta_{\hat{x}} = \frac{V_d}{E_{s0} I_s \lambda_f^{\ 3}} \exp\left(-\lambda_f \hat{x}\right) \cdot \cos\left(\lambda_f \hat{x}\right) \tag{8}$$

where $\hat{x}$ is the distance of the point from the dowel force, I_s is the moment of inertia of the reinforcing bar (for a circular bar with diameter ϕ_s, $I_s = \pi\phi_s^4/64$), and λ_f is a parameter representing the relative stiffness of the foundation (i.e., the surrounding concrete). In the above equation, the value of λ_f is given by

$$\lambda_f = \sqrt[4]{\frac{k_f \phi_s}{4 E_{s0} I_s}} \tag{9}$$

in which k_f is the foundation modulus. Based on experimental results, Dei Poli *et al.* (1992) showed that k_f could vary from 75 to 450 MPa/mm and Soroushian *et al.* (1987) proposed the following formula for k_f

$$k_f = \frac{127\, c_f \sqrt{|f_c|}}{\phi_s^{2/3}} \tag{10}$$

where c_f is a coefficient ranging from 0.6 for a clear bar spacing of 25 mm to 1.0 for larger bar spacing, k_f is expressed in MPa/mm, f_c is expressed in MPa, and ϕ_s is expressed in mm.

The shear deformation of the beam has been neglected in the above classical solution for the beam-on-elastic-foundation problem. Nevertheless, it can be shown using the estimation method given by Essenburg (1962) that for this particular case of steel bars embedded in concrete, the shear deformation is small enough to be regarded as negligible. Hence, the above classical solution with shear deformation neglected is adopted for the derivation of the V_d - Δ_d relation.

Substitute $\hat{x} = 0$ into Eq. (8), the relation between the dowel force and the dowel displacement under elastic condition is obtained as

$$V_d = E_{s0} I_s \lambda_f^{\,3} \Delta_d \tag{11}$$

from which the initial dowel stiffness k_{d0} can be obtained as

$$k_{d0} = E_{s0} I_s \lambda_f^{\,3} \tag{12}$$

On the other hand, the peak dowel force V_{d0} is affected by a number of factors, including the diameter of the dowel bar, embedment length of the dowel bar, concrete cover thickness, concrete strength, steel yield strength and width of concrete member (Jimenez *et al.* 1979). It is not possible, at least at this stage, to take into account all these factors in the estimation of the peak dowel force. For simplicity, the following formula proposed by Vintzeleou and Tassios (1987) is adopted

$$V_{d0} = 1.3\, \phi_s^2 \sqrt{|f_c f_y|} \tag{13}$$

It is noteworthy that Eq. (13) is very similar to that stipulated in CEB-FIP Model Code 1990 (CEB 1993) for a dowel bar subjected to a concentrated dowel force acting right at the shear plane. It is only that in the Model Code 1990 formula, the constant 1.3 in Eq. (13) has been removed and an upper limit of $f_y A_s/\sqrt{3}$ (A_s is the cross-sectional area of the dowel bar) has been imposed on V_{d0}.

The dowel force-displacement relation is well-defined by Eqs. (7), (12) and (13). To formulate

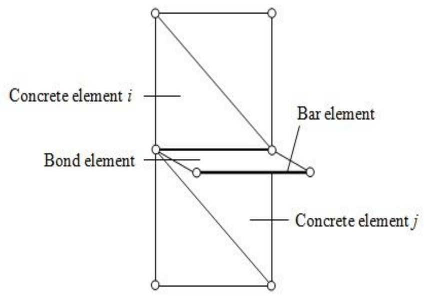

Fig. 6 Adjoining concrete elements

the dowel stiffness matrix, the secant dowel stiffness k_d is evaluated as $E_{s0} I_s \lambda_f^{\ 3}$ using Eq. (12) when the dowel action is still elastic and as V_{d0}/Δ_d using Eq. (13) when the dowel action has become plastic.

4. Modelling of dowel action

In the proposed numerical model for dowel action, the dowel stiffness of the steel reinforcing bars is incorporated into the adjoining concrete elements, so that the steel elements do not need to have flexural stiffness and thereby can be modelled by bar elements with no rotational degrees of freedom. This is done by identifying the concrete elements adjoining each steel element and then superimposing the dowel stiffness matrix onto the stiffness matrices of the adjoining concrete elements. One reason for doing so is that in many existing finite element programs, although the steel reinforcing bars are modelled by discrete one-dimensional elements to allow for bond slip, they are just modelled by bar elements with no rotational degrees of freedom. Another reason is that the dowel force and displacement can actually be transformed into the shear stresses and strains in the adjoining concrete elements, as depicted below.

Consider a dowel bar adjoining two concrete elements, as shown in Fig. 6. The two adjoining concrete elements are numbered as *i* and *j*. The dowel stiffness of the dowel bar is partly apportioned to the concrete element *i* and partly apportioned to the concrete element *j* on a *pro-rata* area basis. Let the area of concrete element *i* be A_i and the area of concrete element *j* be A_j. The dowel stiffness is apportioned to the concrete element *i* according to the distribution coefficient $\alpha_i = A_i/(A_i+A_j)$ and to the concrete element *j* according to the distribution coefficient $\alpha_j = A_j/(A_i+A_j)$.

In the concrete element *i*, the strain vector $[\varepsilon]_i$ can be evaluated as $[B]_i[\delta]_i$ in which $[B]_i$ and $[\delta]_i$ are the strain matrix and displacement vector respectively of the concrete element *i*. By coordinate transformation, the strain vector $[\varepsilon']_i$ in the local coordinate system in which the two coordinate axes are parallel to and perpendicular to the dowel bar can be obtained as

$$[\varepsilon']_i = [T_\Delta][B]_i[\delta]_i \tag{14}$$

In the above equation, $[T_\Delta]$ is the transformation matrix of the dowel bar given by

Table 1 Properties of deep beams analysed

Properties	Specimens			
	NNN-1	NHN-1	NNW-1	NHW-1
Beam breadth (mm)	127.0	127.0	127.0	127.0
Beam depth (mm)	254.0	254.0	254.0	254.0
Effective depth (mm)	215.9	215.9	203.2	198.1
Shear span (mm)	215.9	215.9	203.2	198.1
Span (mm)	431.8	431.8	406.4	396.2
Tensile strength of concrete (MPa)	2.2	3.3	2.1	3.2
Compressive strength of concrete (MPa)	44.6	98.6	40.3	92.8
Tension reinforcement	2 × ϕ19 mm	2 × ϕ19 mm	2 × ϕ19 mm + 2 × ϕ12.8 mm	4 × ϕ19 mm
Compression reinforcement	-	-	2 × ϕ12.8 mm	2 × ϕ12.8 mm
Shear reinforcement	-	-	ϕ6.4 mm @ 101.6 mm c/c	ϕ6.4 mm @ 99.1 mm c/c
Tension reinforcement area (mm^2)	567.7	567.7	825.8	1135.5
Compression reinforcement area (mm^2)	0	0	258.1	258.1
Tension reinforcement ratio (%)	1.8	1.8	2.6	3.5
Compression reinforcement ratio (%)	0	0	0.8	0.8
Yield strength of longitudinal reinforcement (MPa)	420.6	420.6	420.6	420.6
Yield strength of shear reinforcement (MPa)	-	-	324.1	324.1

Note: ϕ means bar diameter while c/c means centre to centre spacing.

$$[T_\Delta] = \begin{bmatrix} c^2 & s^2 & cs \\ s^2 & c^2 & -cs \\ -2cs & 2cs & c^2 - s^2 \end{bmatrix} \tag{15}$$

in which c and s denote respectively the cosine and sine of the angle between longitudinal direction of the dowel bar and the global x-axis. From the local strain vector $[\varepsilon']_i$, the shear strain perpendicular to the dowel bar γ'_i can be extracted and the dowel displacement can be obtained as $\ell_s \gamma'_i$ where ℓ_s is the length of steel bar element. Put together, the dowel displacement is derived as

$$\Delta_d = \ell_s [0 \quad 0 \quad 1][T_\Delta][B]_i [\delta]_i \tag{16}$$

Using the energy principle, the dowel stiffness matrix $[K_{di}]$ of the dowel stiffness apportioned to concrete element i is derived as

$$[K_{di}] = \alpha_i k_d \ell_s{}^2 [B]_i^T [T_\Delta]^T \begin{bmatrix} 0 & 0 & 0 \\ 0 & 0 & 0 \\ 0 & 0 & 1 \end{bmatrix} [T_\Delta][B]_i \tag{17}$$

Likewise, the dowel stiffness matrix $\lfloor K_{dj} \rfloor$ of the dowel stiffness apportioned to concrete element *j* is derived as

$$\left[K_{dj}\right]=\alpha_j k_d \ell_s{}^2 [B]_j^T [T_\Delta]^T \begin{bmatrix} 0 & 0 & 0 \\ 0 & 0 & 0 \\ 0 & 0 & 1 \end{bmatrix} [T_\Delta][B]_j \tag{18}$$

in which the subscript *j* refers to that of the concrete element *j*.

It should be noted that the dowel stiffness matrices given in Eqs. (17) and (18) are each superimposed onto the element stiffness matrix of the respective adjoining concrete element. Hence, the dowel stiffness of the reinforcing bars is incorporated into the adjoining concrete elements and the reinforcing bars can be modelled simply by bar elements. It should also be noted that according to the classical solution for the beam-on-elastic-foundation problem (Hetenyi 1958), the dowel deformation is fairly localised and significant only within a length of $\ell_d = \pi/\lambda_f$. Hence, to properly simulate the dowel action, the length of the steel bar elements ℓ_s must be shorter than ℓ_d.

5. Applications to analysis of deep beams

5.1 Deep beams analysed

The proposed numerical model for the dowel action of discrete reinforcing bars is applied herein to analyse reinforced concrete deep beams tested by others to study its applicability and accuracy. The shear behaviour of deep beams, being a major category of shear critical members, has been researched quite extensively (Smith and Vantsiotis 1982, Hwang *et al.* 2000, Russo *et al.* 2005). Basically, it has been found that the dowel action of reinforcing bars can play an important role in the shear behaviour of deep beams, especially when the amount of shear reinforcement provided is relatively small (He and Kwan 2001). Furthermore, since the dowel action becomes more fully developed after the concrete beam has cracked and can last until the whole concrete beam has failed, its contribution to the shear resistance of the concrete beam increases as the beam cracks and enters into the post-peak stage. Hence, the dowel action of reinforcing bars may contribute significantly to the shear strength and ductility of the concrete beam.

The beams chosen to be analysed by the proposed discrete reinforcing bar and dowel action model are the deep beam specimens NNN-1, NHN-1, NNW-1 and NHW-1 tested by Xie *et al.* (1994). These deep beams have been analysed before by He (1999) using the old fashioned smeared reinforcement approach. Fig. 7 and Table 1 present the geometric layout, reinforcement details and material properties of the deep beams. The four deep beam specimens have the same cross-sections of 127.0 mm breadth by 254.0 mm depth. Because of the difference in longitudinal reinforcement, the deep beam specimens NNN-1, NHN-1, NNW-1 and NHW-1 have effective depths of 215.9 mm, 215.9 mm, 203.2 mm and 198.1 mm, respectively. They were each subjected to a single point load acting at mid-span. The shear span to effective depth ratios (a_v/d) of the four beam specimens were all fixed at 1.0.

The first two specimens were singly-reinforced with no stirrups provided while the latter two specimens were doubly-reinforced with stirrups provided as shear reinforcement. The first and

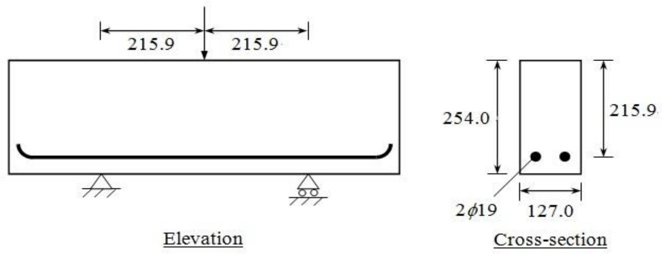

(a) Specimens NNN-1 and NHN-1

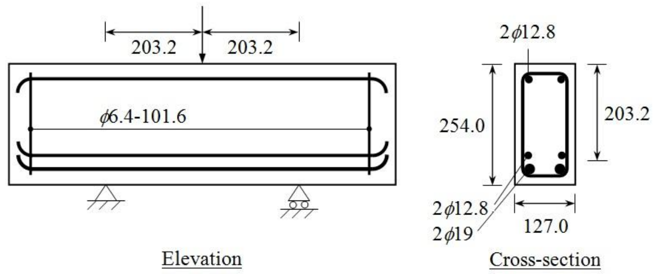

(b) Specimen NNW-1

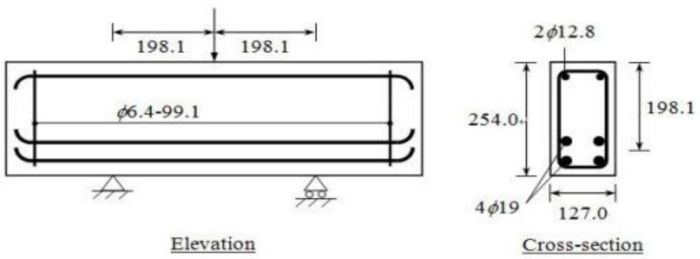

(c) Specimen NHW-1

Fig. 7 Deep beam specimens analysed (dimensions in mm)

third specimens were cast of normal-strength concrete with f_c slightly higher than 40 MPa whereas the second and fourth specimens were cast of high-strength concrete with f_c slightly higher than 90 MPa. The yield strengths of the longitudinal and shear reinforcements were 420.6 MPa and 324.1 MPa, respectively. The elastic modulus and coefficient n of the reinforcing steel were not reported and are assumed to be 200 GPa and 2.0, respectively. For the longitudinal reinforcement, which is modelled by discrete bar elements, the ultimate tensile strength, strain at start of strain hardening and ultimate strain are taken as 740 MPa, 1.0% and 12.0%, respectively. For the shear reinforcement, which is modelled as smeared reinforcement, the ultimate tensile strength, strain at start of strain hardening and ultimate strain are taken as 540 MPa, 2.1% and 16.7%, respectively. For the bond between steel reinforcement and concrete, the material parameters pertinent to deformed bars recommended in Model Code 1990 are adopted. Accordingly, the peak bond stress τ_p and residual bond stress τ_f are taken as $2.0f_c^{0.5}$ and $0.3f_c^{0.5}$, respectively, and the slip parameters s_1, s_2 and s_3 are taken as 0.6 mm, 0.6 mm and 1.0 mm, respectively.

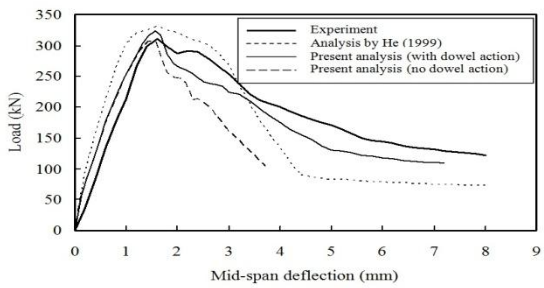

(a) Specimen NNN-1

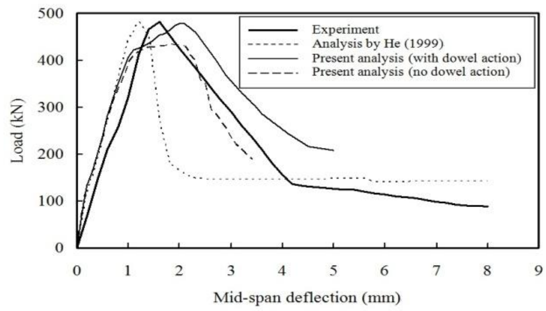

(b) Specimen NHN-1

Fig. 8 Load-deflection curves of Specimens NNN-1 and NHN-1

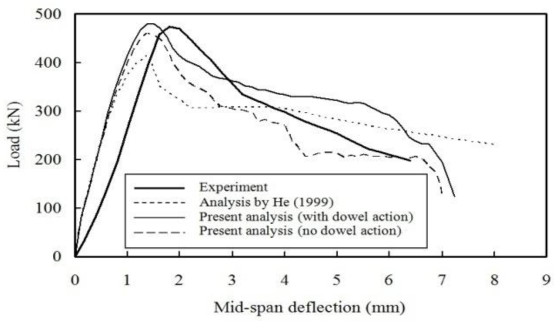

(a) Specimen NNW-1

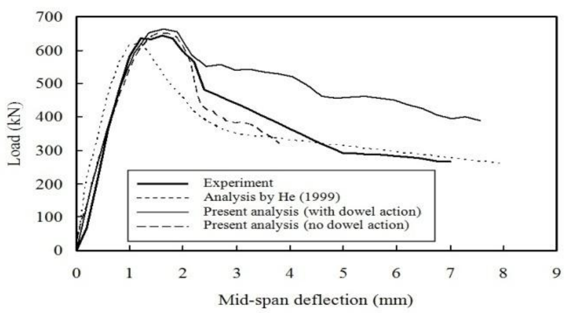

(b) Specimen NHW-1

Fig. 9 Load-deflection curves of Specimens NNW-1 and NHW-1

5.2 Results and discussions

The above deep beam specimens are each analysed twice, first with the dowel action of discrete reinforcing bars ignored and again with the dowel action of discrete reinforcing bars incorporated. The analytical load-deflection curves so obtained are compared to the corresponding experimental load-deflection curves by Xie *et al.* (1994) and the computed load-deflection curves by He (1999) using the smeared reinforcement approach in Figs. 8 and 9. Xie *et al.* reported the experimental peak loads of NNN-1, NHN-1, NNW-1 and NHW-1 as 311.5 kN, 483.0 kN, 473.7 kN and 645.0 kN, respectively. From these peak load values, the effects of using high-strength concrete and/or providing compression and shear reinforcements on shear strength may be assessed as follows. By using high-strength concrete to cast the deep beam, the peak load was increased by 55% (NHN-1 versus NNN-1) when shear reinforcement was not provided and by 36% (NHW-1 versus NNW-1) when shear reinforcement was provided. Furthermore, by providing compression and shear reinforcements, the peak load was increased by 52% (NNW-1 versus NNN-1) for normal-strength concrete deep beam and by 34% (NHW-1 versus NHN-1) for high-strength concrete deep beam.

The analytical peak loads of NNN-1, NHN-1, NNW-1 and NHW-1 obtained with the dowel action of discrete reinforcing bars ignored are 306.7 kN, 433.9 kN, 459.2 kN, and 650.5 kN, respectively. The first three analytical peak loads are slightly lower than the respective experimental values whereas the last analytical peak load is almost the same as the respective experimental value. Although these analytical peak loads seem to agree quite closely with the experimental results, the analytical load-deflection curves, as shown in Figs. 8 and 9, do not agree well with the experimental load-deflection curves. Basically, the analytical load-deflection curves with the dowel action of discrete reinforcing bars ignored agree well with the respective experimental load-deflection curves only at the pre-peak stage and are significantly lower than the respective experimental load-deflection curves at the post-peak stage. Overall, the analytical load-deflection curves with the dowel action ignored show a more brittle failure mode than that observed in the experiments.

The analytical peak loads of NNN-1, NHN-1, NNW-1 and NHW-1 obtained with the dowel action of discrete reinforcing bars incorporated are 323.8 kN, 478.1 kN, 479.1 kN, and 664.1 kN, respectively. These analytical peak loads match very closely with the respective experimental values. Furthermore, as shown in Figs. 8 and 9, the analytical load-deflection curves agree reasonably well with the experimental load-deflection curves at both the pre-peak and post-peak stages. Relatively, the analytical load-deflection curves agree better with the respective experimental load-deflection curves at the pre-peak stage than at the post-peak stage. At the post-peak stage, the analytical load-deflection curves sometimes appear to be quite erratic because of occasional numerical instability during the analysis of the deep beams at the post-peak stage. Another problem is that for the deep beams cast of high-strength concrete, the analytical load-deflection curves are somewhat higher than the respective experimental load-deflection curves at the post-peak stage, indicating a more ductile failure mode than that observed in the experiments.

Overall, it may be said that with the dowel action ignored, the analytical peak load would tend to be slightly lower than the experimental value and the analytical load-deflection curve would at the post-peak stage become significantly lower than the experimental curve showing a more brittle failure mode than the reality. With the dowel action incorporated, the analytical peak load would be closer to the experimental value and the analytical load-deflection curve would agree better with the experimental curve. Hence, the dowel action of reinforcing bars should always be taken into account in the finite element analysis. However, for high-strength concrete beams, the

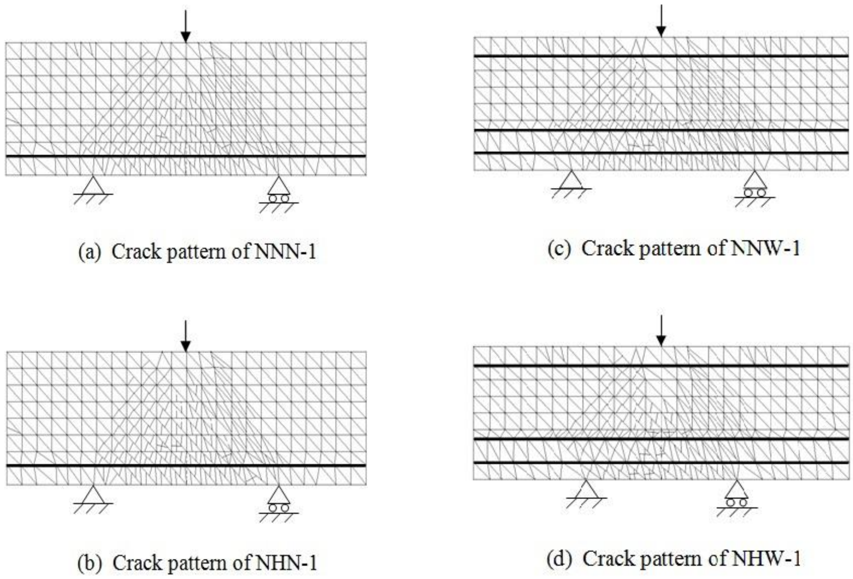

Fig. 10 Crack patterns of deep beam specimens

analytical load-deflection curve with the dowel action incorporated would tend to be higher than the experimental curve at the post-peak stage, indicating a more ductile failure mode than the reality. One main reason is that although in reality the high-strength concrete should be more brittle than the normal-strength concrete, in the finite element analysis, the high-strength concrete and normal-strength concrete were assumed to have stress-strain curves with similar shape and ductility (only the strength values are different). To resolve this problem, it is recommended that for concrete, stress-strain curves reflecting gradual reduction in ductility as strength increases should be used instead.

The computed load-deflection curves obtained by He (1999) using the smeared reinforcement approach are also plotted in Figs. 8 and 9 for comparison. In He's analysis, the reinforcing bars were smeared within the concrete elements assuming perfect bond between the reinforcing bars and the surrounding concrete. Hence, the bond slip of the reinforcing bars was neglected. Nevertheless, the dowel action of the reinforcing bars was allowed for using a dowel action model similar to the present one (He and Kwan 2001). From He's computed load-deflection curves, it can be seen that the computed peak loads match quite closely with the experimental results but the computed load-deflection curves do not agree well with the experimental load-deflection curves at the post-peak stage. Particularly, the computed load-deflection curve often descends more rapidly than the respective experimental load-deflection curve indicating a smaller deformability of the deep beams than that observed in the experiments. An obvious reason is that in He's analysis, the bond slip of the reinforcing bars has been neglected and, as a result, the deflection of the deep beam at the post-peak stage tended to be underestimated and the deep beam failed at a relatively small deflection. Hence, the smeared reinforcement approach, which is not capable of accounting for the bond slip of the reinforcing bars, is not desirable.

Lastly, the crack patterns obtained by the present analysis with the dowel action incorporated are displayed in Fig. 10. The cracks are nearly vertical near the mid-span location and are generally more inclined closer to the supports. Right at the supports, the cracks are inclined at approximately 45° to the vertical. Furthermore, the finite element analysis results reveal the following structural actions. Between the inclined cracks extending from the loading point to the supports, concrete struts are formed. The concrete struts are subjected to compression and the lower end of each concrete strut tends to move laterally outward. The longitudinal reinforcing bars at the bottom of the beam tie back the concrete struts to prevent the lateral outward movement of the lower ends of the concrete struts. Because of such tie back action, bond slip between the longitudinal reinforcing bars and the surrounding concrete occurs near the supports. At the same time, the portion of concrete underneath the inclined cracks moves downward. This causes the shear reinforcement to develop tension and the longitudinal reinforcing bars crossing the inclined cracks to develop dowel action to hold back the downward movement of the concrete. Shear sliding along the inclined cracks also occurs and thus the inclined cracks are not purely tension cracks. Summing up, it may be concluded that for a reinforced concrete deep beam, the bond slip of reinforcing bars, the dowel action of reinforcing bars and the aggregate interlock against shear sliding of cracks are all important. Proper modelling of all these structural actions is needed for finite element analysis.

6. Conclusions

In the finite element analysis of concrete structures, discrete representation of the steel reinforcing bars is a more realistic way to reflect the interactions between the reinforcement and the surrounding concrete than smeared representation. There are several reasons. First, the positions of the reinforcing bars are more precisely defined. Second, the bond slip of the reinforcing bars can be allowed for. Third, the dowel action of the reinforcing bars can be more appropriately modelled. However, as the dowel action is accompanied by flexural deformation, the reinforcing bars should in theory be modelled by frame elements with rotational degrees of freedom. Herein, a dowel action model for discrete reinforcing bars, in which the dowel stiffness of the reinforcing bars is incorporated into the adjoining concrete elements so that the reinforcing bars can be modelled simply by bar elements with no rotational degrees of freedom, is developed. The beam-on-elastic-foundation theory is employed to derive the dowel stiffness and an existing formula based on experimental results is used to derive the dowel strength. This dowel action model has been incorporated in a finite element program based on secant stiffness formulation for post-peak analysis of concrete structures.

The above finite element program has been applied to the analysis of deep beams with well documented experimental results. Numerical results verified that the incorporation of both the dowel action and the bond slip of the reinforcing bars would significantly improve the accuracy of the analysis, not only in terms of the peak load but also in terms of the load-deflection curve at pre-peak and post-peak stages. Generally, with the dowel action taken into account, the ductility of the deep beam would be more accurately revealed and with the bond slip taken into account, the deformability of the deep beam would be better simulated. From the finite element analysis results, the following structural actions in deep beams are observed: (1) concrete struts are formed between the inclined cracks extending from the loading point to the supports; (2) bond slip occurs mainly in the longitudinal reinforcement near the supports; (3) dowel action occurs mainly in the longitudinal reinforcement crossing the inclined cracks; and (4) shear sliding occurs along the inclined cracks. Hence, for deep beams, the bond slip of reinforcing bars, dowel action of reinforcing bars and aggregate interlock against shear sliding of cracks are all important and should be properly modelled.

References

ASCE Task Committee on Finite Element Analysis of Reinforced Concrete Structures (1982), "State-of-the-Art Report on Finite Element Analysis of Reinforced Concrete Structures", ASCE, New York, USA.

Bresler, B. and Scordelis, A.C. (1963), "Shear strength of reinforced concrete beams", *ACI J.*, **60**(1), 51-74.

Comite Euro-International du Beton (1993), CEB-FIP Model Code 1990: Model Code for Concrete Structures, Thomas Telford, London, UK.

Dei Poli, S., Di Prisco, M. and Gambarova, P.G. (1992), "Shear response, deformations, and subgrade stiffness of a dowel bar embedded in concrete", *ACI S. J.*, **89**(6), 665-675.

Dei Poli, S., Di Prisco, M. and Gambarova, P.G. (1993), "Cover and stirrup effects on the shear response of dowel bar embedded in concrete", *ACI S. J.*, **90**(4), 441-450.

Dulacska, H. (1972), "Dowel action of reinforcement crossing cracks in concrete", *ACI J.*, **69**(12), 754-757.

El-Ariss, B. (2007), "Behavior of beams with dowel action", *Eng. Struct.*, **29**(6), 899-903.

Essenburg, F. (1962), "Shear deformation in beams on elastic foundations", *J. Appl. Mech.*, ASME, **29**, 313-317.

Goodman, R.E., Taylor, R.L. and Brekke, T.L. (1968), "A model for the mechanics of jointed rock", *J. Soil Mech. Found. Division*, ASCE, **94**(3), 637-659.

Guo, Z.H. and Zhang, X.Q. (1987), "Investigation of complete stress-deformation curves for concrete in tension", *ACI Mater. J.*, **84**(4), 278-285.

Hassan Dirar, S.M.O. and Morley, C.T. (2005), "Nonlinear finite element analysis of reinforced concrete deep beams", (Eds. Onate, E. and Owen, D.R.J.), *Proceedings of the 8th International Conference on Computational Plasticity, Barcelona*, Spain.

He, X.G. (1999), "Constitutive modeling of reinforced concrete for nonlinear finite element analysis", Ph.D. Thesis, The University of Hong Kong, Hong Kong.

He, X.G. and Kwan, A.K.H. (2001), "Modeling dowel action of reinforcement bars for finite element analysis of concrete structures", *Comput. Struct.*, **79**(6), 595-604.

Hetényi, M.I. (1958), *Beams on Elastic Foundation: Theory with Applications in the Fields of Civil and Mechanical Engineering*, The University of Michigan Press, Ann Arbor, USA.

Hwang, S.J., Lu, W.Y. and Lee, H.J. (2000), "Shear strength prediction for deep beams", *ACI Struct. J.*, **97**(3), 367-376.

Jimenez, R., White, R.N. and Gergely, P. (1979), "Bond and dowel capacities of reinforced concrete", *ACI J.*, **76**(1), 73-92.

Kazaz, I. (2011), "Finite element analysis of shear-critical reinforced concrete walls", *Comput. Concrete*, **8**(2), 143-162.

Krefeld, W.J. and Thurston, C.W. (1966), "Contribution of longitudinal steel to shear resistance of reinforced concrete beams", *ACI J.*, **63**(3), 325-344.

Kupfer, H.B. and Gerstle, K.H. (1973), "Behavior of concrete under biaxial stresses", *J. Eng. Mech. Division*, ASCE, **99**(4), 853-866.

Kwak, H.G. and Kim, D.Y. (2004), "FE analysis of RC shear wall subject to monotonic loading", *Mag. Concrete Res.*, **56**(7), 387-403.

Mander, J.B. (1984), "Seismic Design of Bridge Piers", Ph.D. Thesis, University of Canterbury, New Zealand.

Mannava, S.S., Bush, T.D. and Kukreti, A.R. (1999), "Load-deflection behavior of smooth dowels", *ACI Struct. J.*, **96**(6), 891-898.

Millard, S.G. and Johnson, R.P. (1984), “Shear transfer across cracks in reinforced concrete due to aggregate interlock and dowel action”, *Mag. Concrete Res.*, **36**(126), 9-21.

Ng, P.L. (2007), “Constitutive modelling and finite element analysis of reinforced concrete structures”, Ph.D. Thesis, The University of Hong Kong, Hong Kong.

Oliveira, R.S., Ramalho, M.A. and Correa, M.R.S. (2008), “A layered finite element for reinforced concrete beams with bond-slip effects”, *Cement Concrete Compos.*, **30**(3), 245-252.

Park, R. and Paulay, T. (1975), *Reinforced Concrete Structures*, John Wiley & Sons, New York, USA.

Pimentel, M., Cachim, P. and Figueiras, J. (2008), “Deep-beams with indirect supports: numerical modelling and experimental assessment”, *Comput. Concrete*, **5**(2), 117-134.

Pruijssers, A.F. (1988), “Aggregate interlock and dowel action under monotonic and cyclic loading”, Ph.D. Thesis, Delft University of Technology, Netherland.

Russo, G., Venir, R. and Pauletta, M. (2005), “Reinforced concrete deep beams-shear strength model and design formula”, *ACI Struct. J.*, **102**(3), 429-437.

Saenz, L.P. (1964), “Discussion of the paper ‘Equation for the stress-strain curve of concrete’ by Prakash Desayi and S. Krishman”, *ACI J.*, **61**(9), 1229-1235.

Smith, K.N. and Vantsiotis, A.S. (1982), “Shear strength of deep beams”, *ACI J.*, **79**(3), 201-213.

Soroushian, P., Obaseki, K., Baiyasi, M.I., El-Sweidan, B. and Choi, K.B. (1988), “Inelastic cyclic behavior of dowel bars”, *ACI Struct. J.*, **85**(1), 23-29.

Soroushian, P., Obaseki, K., Rojas, M.C. and Najm, H.S. (1987), “Behavior of bars in dowel action against concrete cover”, *ACI Struct. J.*, **84**(2), 170-176.

Soroushian, P., Obaseki, K., Rojas, M.C. and Sim, J.S. (1986), “Analysis of dowel bars acting against concrete core”, *ACI J.*, **83**(4), 642-649.

Vintzeleou, E.N. and Tassios, T.P. (1986), “Mathematical models for dowel action under monotonic and cyclic conditions”, *Mag. Concrete Res.*, **38**(134), 13-22.

Vintzeleou, E.N. and Tassios, T.P. (1987), “Behavior of dowels under cyclic deformations”, *ACI Struct. J.*, **84**(1), 18-30.

Walraven, J.C. (1980), “Aggregate interlock: a theoretical and experimental analysis”, Ph.D. Thesis, Delft University of Technology, Netherlands.

Xie, Y.L., Ahmad, S.H., Yu, T.J., Hino, S. and Chung, W. (1994), “Shear ductility of reinforced concrete beams of normal and high-strength concrete”, *ACI Struct. J.*, **91**(2), 140-149.

Yu, R.C., Saucedo, L. and Ruiz, G. (2011), “Finite-element study of the diagonal-tension failure in reinforced concrete beams”, *Int. J. Fracture*, **169**(2), 169-182.

Zhao, Z.Z., Kwan, A.K.H. and He, X.G. (2004), “Nonlinear finite element analysis of deep reinforced concrete coupling beams”, *Eng. Strcut.*, **26**(1), 13-25.

CC